Anritsu envision : ensure

Performing Differential Noise Figure Measurements

VectorStar™ MS4640B Series Vector Network Analyzer, Option 48

Overview

In recent years, numerous improvements have been made in noise figure measurements through better algorithmic understanding of the measurements (e.g., [1]-[6]), more sensitive receivers, and less error-prone methods of processing noise power measurements. Anritsu has incorporated a number of these improvements in the single-ended Noise Figure Measurement Option (Option 41) of the VectorStar vector network analyzer (VNA) platform.

Another wave of improvements in noise figure is the increased proliferation of differential low-noise amplifiers (LNAs). Until now, noise figure measurements have only addressed the needs of the single-ended community and have not offered a well-defined approach to noise figure analysis of differential devices. The introduction of the VectorStar Differential Noise Figure option allows the VNA to measure 3- and 4-port devices in single-ended, differential, and common mode operation with a variety of processing options.

One of the earlier improvements is the incorporation of the cold-source noise figure measurement method commonly used with VNAs. It is one of the two common noise figure measurement methods (the other is the hot-cold or Y-factor method). The Anritsu differential noise figure option incorporates the similar cold-source measurement technique as its 2-port method, which minimizes mismatch errors for improved accuracy compared to the conventional Y-factor noise source method. The new enhanced noise figure option adds the ability to perform levels of vector correction in both 2-port and multi-port devices for even greater accuracy particularly when mismatch is significant.

This application note offers insights in to and examples of performing differential noise figure measurements. However, it would be beneficial to first review the differences in the Y-factor and cold-source methods before going in-depth in to a description of differential measurements.

Y-Factor (Hot-Cold) Noise Figure Measurement Method

The Y-factor method was popular for noise figure measurements that used a noise source that could produce a low noise output power (cold = N_c) and an elevated one (hot=N_h). This noise source would then become the input noise signal to the device under test (DUT). The ratio of measured noise powers in these two states was termed the Y-factor (e.g. [2]) ($Y=N_h/N_c$) and could lead to a quick calculation of noise figure via the equation (Eq. 1) below.

$$F = \frac{\frac{T_h}{T_0} - 1}{Y - 1} \quad (1)$$

Where Th is the equivalent hot temperature of the noise source and the cold temperature was assumed equal to a room temperature of 290K=T_0. By making a noise figure measurement of the receiver itself and of the system (DUT + receiver), it was possible to deconvolve the DUT noise figure with the Friis' equation (Eq. 2) below: [1]

$$F_{DUT} = F_{Sys} - \frac{F_{rcvr}-1}{G} \quad (2)$$

Here the DUT gain, G, could be measured separately (via S-parameters) or it could be determined from the change in measured noise powers during calibration and measurement. One advantage the Y-factor noise figure measurement method had was that no absolute power calibrations were needed (all based on ratios). This was particularly important in the past when wide dynamic range power measurements over large bandwidths were more difficult.

Issues common to the Y-factor method were calibration and mismatch errors. The noise source used in the Y-factor method needs to be periodically calibrated in order to confirm accuracy of measurement. This then takes the place of using a calibrated power meter as the reference. In addition, mismatch errors become a significant consideration due to the match changes of the source when switching between the hot and cold states [4]. This could lead to large errors, particularly as the DUT input match worsened and significant effort was not made to correct.

Cold-Source Noise Figure Measurement Method

The cold-source noise figure measurement method was developed to eliminate the requirement for a multi-state noise source, which would allow the use of a simpler, better controlled noise source (nominally a termination at room temperature). In this case, the noise figure is found from a more easily populated equation (Eq. 3), but it has some subtleties:

$$F = \frac{kT_0B+N}{kT_0BG} \quad (3)$$

Here:
- k is Boltzmann's constant
- N is the noise power added
- G is the gain
- B is the bandwidth

To calculate the noise figure, there are a few key steps that must be taken. First, an absolute noise power is now required (numerator N), so a means of a receiver power calibration is needed. Anritsu's highly accurate power calibrations and very linear broadband receiver facilitate this. Other methods are possible to determine added noise power, including the use of a calibrated hot noise source (only during the calibration step), however in both cases an absolute power reference is being created. Second, an effective measurement bandwidth (B) is needed. Since measurement bandwidth is largely determined by the digital IF system of the VNA, B can be pre-determined. This bandwidth value may also be determined in the absolute power calibration step if a noise source is used. Third, to isolate the noise figure of the DUT, the noise contributions of the receiver must be taken into account. As with the hot-cold method, a measurement of receiver noise is required, this time only with the cold-source attached to the receiver input. Taking the receiver noise into account, Eq. 3 above can be re-expressed in the form below (Eq. 4):

$$F = \frac{1}{G} + \frac{N_{DUT+rcvr} - N_{rcvr}}{kT_0BG} \quad (4)$$

A few things are immediately obvious: errors in gain or the noise power measurement will propagate to noise figure on roughly a dB-for-dB basis (if the composite receiver gain is sufficiently high). These accuracies will be discussed throughout this application note, but it is worth remembering the approximate dependence.

Anritsu's Differential Noise Figure Option (Option 48) is an enhancement of, and exclusive of, the Noise Figure Option (Option 41). Option 48 includes the ability to handle: 3- and 4-port DUTs in a single-ended sense; differential and common mode noise figure for all DUTs with a variety of processing options; and, the inclusion of a level of vector match correction to enhance accuracy. The menu system is augmented to help speed the calibration procedures. The basic measurement process (that of cold-source analysis) remains the same, as do most of the guiding principles on the receiver preamplifier/filtering.

Much work has been published in the area of differential noise figure (e.g., [1]-[7]), although there is still some inconsistency on terminology and on measurement approaches. This application note does not attempt to resolve these issues, but is instead intended to suggest one way forward that potentially has some practical advantages, is largely self-consistent, and can lead to some reasonable measurement results in a wide range of DUT configurations.

Multiport DUTs: Gain Aspects

Handling of the DUT gain is an important part of noise figure computations and, in the case of 3- and 4-port DUTs, the S-parameters will come in the form of an .s3p or .s4p file. If the DUT outputs are to be treated as single-ended, then the analysis process may just be a simple extraction of the 2-port paths of interest. If it is to be treated as a differential or common-mode measurement, then the gain must be calculated in those terms. To further complicate the practicalities, the port assignment in the .s3p/.s4p file may not match how the DUT is connected to the noise measurement ports.

Port Assignments

The DUT S-parameter file loader in noise figure always uses the following port assignment for .s4p: DUT inputs are ports 1 and 2 connected, respectively, to output ports 3 and 4. When loading the file, a port swap tool is available to let the user align the port configuration used in the actual file to the port assignment (shown in Figure 1) used by the noise figure application.

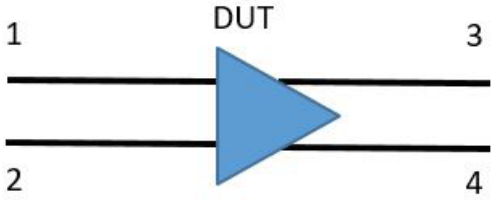

Figure 1. Port Assignments When Loading .s4p Files for DUT S-parameters. If the data was saved using a different port configuration, there is a port reassignment tool available.

For the .s3p case with an output pair, the following assignment is ALWAYS used: ports 2 and 3 form the output (Figure 2).

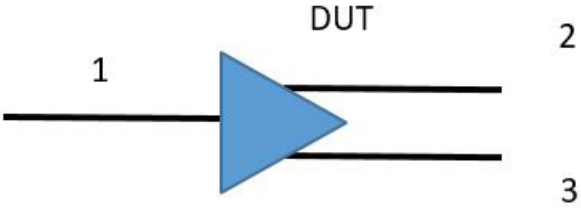

Figure 2. Port Assignments When Loading .s3p Files for DUT S-parameters. If the data was saved using a different port configuration, there is a port reassignment tool available.

Gain Definitions

For differential insertion gain, the mixed-mode parameter S_{d2d1} is used. The mode conversion parameter S_{d2c1} is also needed and the net insertion gain is $|S_{d2d1}|^2 + |S_{d2c1}|^2$. Similarly for common-mode, the net insertion gain is $|S_{c2c1}|^2 + |S_{c2d1}|^2$. The concept on these gain configurations relies on the use of uncorrelated terminations at temperature T_0. While this will be discussed further from a gain perspective, what this means is that equal noise inputs at the common- and differential modes will exist. Thus, the gain of interest has to take into account the output power in a given mode due to both differential and common-mode noise inputs. The mixed-mode parameters for the port assignments shown above are defined here as:

$$S_{d2d1} = \frac{1}{2}(S_{31} + S_{42} - S_{32} - S_{41})$$

$$S_{d2c1} = \frac{1}{2}(S_{31} - S_{42} + S_{32} - S_{41})$$

$$S_{c2c1} = \frac{1}{2}(S_{31} + S_{42} + S_{32} + S_{41})$$

$$S_{c2d1} = \frac{1}{2}(S_{31} - S_{42} - S_{32} + S_{41}) \quad (5)$$

For the 3-port case with a mixed-mode DUT output, there are no mode conversion issues and the insertion gains are $|S_{d1}|^2$ and $|S_{c1}|^2$ for differential and common-mode respectively. The mixed-mode definitions of the underlying parameters are:

$$S_{d1} = \frac{1}{\sqrt{2}}(S_{21} - S_{31})$$

$$S_{c1} = \frac{1}{\sqrt{2}}(S_{21} + S_{31}) \quad (6)$$

The use of available gain is more correct for noise figure analysis, as has been discussed previously, and the multiport equivalent of this added level of vector correction is also available. These definitions are in Eq. 7 and, as in the 2-port case, account for the power delivery impact of DUT output mismatch.

$$G_{diff,avail} = \frac{(|S_{d2d1}|^2 + |S_{d2c1}|^2)}{1 - |S_{d2d2}|^2}$$

$$G_{cm,avail} = \frac{(|S_{c2c1}|^2 + |S_{c2d1}|^2)}{1 - |S_{c2c2}|^2} \quad (7)$$

For the SE-in, diff out 3-port DUT case, things simplify:

$$G_{diff,avail,SEin-DiffOut} = \frac{(|S_{d1}|^2)}{1 - |S_{dd}|^2}$$

$$G_{cm,avail,SEin-CmOut} = \frac{(|S_{c1}|^2)}{1 - |S_{cc}|^2} \quad (8)$$

The underlying definitions for the reflection mixed-mode parameters used here are (again DUT output ports) 3 and 4 for the 4-port case and 2 and 3 for the 3-port case:

$$S_{d2d2} = \frac{1}{2}(S_{33} + S_{44} - S_{34} - S_{43})$$

$$S_{c2c2} = \frac{1}{2}(S_{33} + S_{44} + S_{34} + S_{43})$$

$$S_{dd} = \frac{1}{2}(S_{33} + S_{22} - S_{23} - S_{32})$$

$$S_{cc} = \frac{1}{2}(S_{33} + S_{22} + S_{23} + S_{32}) \quad (9)$$

For 2-port DUT analysis, the available gain used is $|S_{21}|^2/ (1-|S_{22}|^2)$ where 1->2 is the path of analysis.

Multiport DUTs: Network Extraction Aspects

As with 2-port noise figure, it may be desirable to embed or de-embed networks from the measurement (probes, for example). With multiport DUTs, the networks to be added/subtracted can also be multiport, so some logistical complications arise as with gain. .s2p files are always supported and are embedded or de-embedded in a simple single-ended sense where one file is associated with each port pair. For an .s4p file, the paths will be treated as single-ended as well since mode-conversion calculations at this stage are prone to error. The user can specify which path in the file should be associated with the b_1 receiver and the disjoint path will automatically be used for the b_2 receiver.

Example: A differential probe is used and the .s4p file has dominant paths 1->2 and 3->4 (i.e., the low insertion loss parameters are S_{21}, S_{12}, S_{43}, and S_{34}). The user cables what is nominally port 2 of the probe to the b_1 receiver chain. On the network extraction dialog, the user should select 1->2 as the path for the VNA b_1 receiver. This will result in S_{21} being used for embedding/de-embedding on the b_1 noise data and S_{43} will be used on b_2 noise data.

Multiport DUTs: Noise Measurement Background

Noise figure definitions present some interesting challenges, particularly in a multiport context. To start, consider the IEEE definition, which is somewhat intrinsically 2-port. It relies on the noise power out of a DUT when the input is terminated, in a reflection-less way, with a body at T_0=290K.

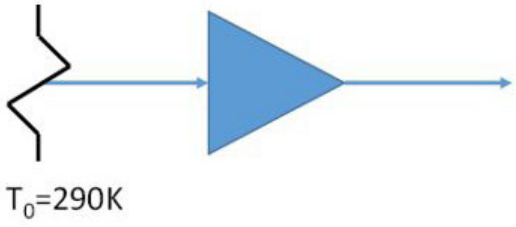

Figure 3. Classical Configuration Assumed for 2-port Noise Figure Measurements. The input termination is assumed to be noisy but reflection-less.

Now, as has been discussed in the literature [1], the multiport situation raises some questions:

- Can we segregate ports into 'input' and 'output' classes?
- How are the input ports terminated? Are all at T_0 or are all but one 'noiseless'? If all are noisy, are those noise signals correlated? Does it matter if the distribution of input noise is by port or by mode?
- If measuring noise at output port M, how is output port N terminated? Can the output port be terminated indirectly (e.g., through a probe) with minimal accuracy impact?

How are noise parameter inputs to be thought of? A vector of input impedances and an input correlation matrix?

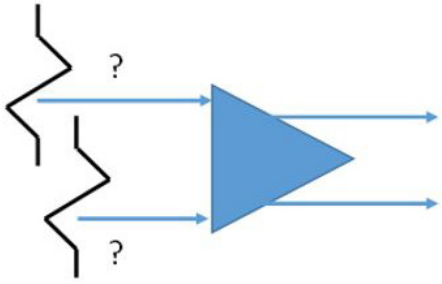

Figure 4. Choosing the Noise Figure Definition for a Differential Device. For a differential device (or for a multiport DUT in general), the existing noise figure definitions are somewhat incomplete, but reasonable choices can be made.

The input/output assignment question ends up having little practical impact. For a passive DUT, one can assign these on the fly, and for an active DUT it generally follows logically: those ports that have gain to some other port should be terminated in T_0. As we will see later, the passive network case ends up being less confusing than it might seem.

Why should we terminate the inputs in noisy T_0 terminations? One could generate a more detailed picture of a DUT by using some noiseless terminations and other combinations, but recall that noise figure is generally intended to represent a simple way (with a single value) of expressing the noise output of a DUT under some representative conditions. The more complete description is left to noise parameters. Practically speaking, it would be hard to apply noiseless terminations to certain ports for measurement and would not represent many practical use cases anyway. Extending the 2-port definition makes sense in this way. The next question is one of correlation of the inputs (and there will be much more on this later): should the input noise sources be uncorrelated or correlated in some manner? Going back to the concept of noise figure as a single number, it would seem to make sense to have the inputs be uncorrelated since: (a) that is practical from a measurement perspective, (b) it is the most easily described configuration, and (c) the correlated case is best handled in the realm of noise parameters since there is an arbitrarily large number of possible correlated inputs.

The output port terminations again go back to the question of assignment. In the case of a device with gain, the terminations on the output ports not being measured are going to have little practical impact (assuming the DUT doesn't oscillate in this case). In the case of a passive network, all ports not being measured should be assigned the state of “input” and be appropriately terminated for the definitions to be consistent.

Before going further, it may be helpful to revisit the concept of correlation. Mathematically, the cross-correlation of two signals is simply (where * denotes complex conjugate)

$$\rho_{12} = \sum_i b_1(i) b_2^*(N-i) \tag{10}$$

Multiport DUTs: Noise Measurement Background

Where N is some positional index that might reveal some information when two signals are related but shifted relative to each other. In general, if b_1 and b_2 are noise signals from independent sources (and have zero mean), one would expect this sum to be very small in the limit of many samples since each individual $b_1 b_2$ product will be randomly phased. If, however, the two noise signals are derived from the same source, there would tend to be some common phase relationship between b_1 and b_2, so the product terms will all tend to align and the sum becomes non-zero. This is the result for two correlated noise signals.

Consider next a passive network (with T-terminated inputs) at temperature T. Ignore all reflections and connect an ideal, lossless hybrid at the output so we have some final output signals ~b_1 and ~b_2. This line of analysis was reported in [2].

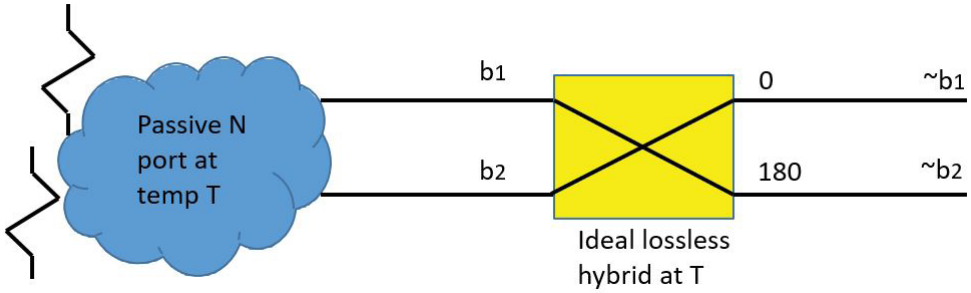

Figure 5. Noise Correlation Behavior in Passive Multiport at Thermal Equilibrium.

A measurement thought experiment (after [2]) is sketched here to illustrate noise correlation behavior in a passive multiport at thermal equilibrium.

Because everything is at temperature T (and is presumably at equilibrium), the noise powers in the various output places must be the same and equal to kTB, where k is Boltzmann's constant and B is the measurement bandwidth.

$$\overline{|b_1|^2} = \overline{|b_2|^2} = \overline{|{\sim}b_1|^2} = \overline{|{\sim}b_2|^2} = kTB \tag{11}$$

Here the overbars indicate mean summation. From Figure 5, $\sim b_1$ and $\sim b_2$ must represent the sum and difference, respectively, of b_1 and b_2. But because of the ideality of the hybrid, those output noise powers must also satisfy

$$\overline{|{\sim}b_1|^2} = \frac{1}{2}\left(\overline{|b_1|^2} + \overline{|b_2|^2}\right) + Re\left(\overline{b_1 \cdot b_2^*}\right)$$

$$\overline{|{\sim}b_2|^2} = \frac{1}{2}\left(\overline{|b_1|^2} + \overline{|b_2|^2}\right) - Re\left(\overline{b_1 \cdot b_2^*}\right) \tag{12}$$

The only way both equations Eq. 12 can be true is if $Re(b_1 \cdot b_2^*)=0$. But this is just the real projection of correlation. If we repeat this thought experiment with a 90 degree hybrid instead of a 180 degree hybrid, we will reach the conclusion that $Im(b_1 \cdot b_2^*)=0$. This interesting result (called Bosma's theorem) is that noise power emanating from a passive multiport must be uncorrelated. Not only does this lend some further justification to our noise figure definition, but it also makes it practically much easier to analyze the effects of network losses before the DUT (probes, pads, etc.): they do not induce any input correlation.

In terms of an actual active DUT noise figure measurements, what are then the impacts of correlation? On one level are the users' system implications: how will the DUT outputs be used? If they end up feeding single-ended receivers, it may not matter much. If they feed another stage in a fully differential system, it may matter quite a lot. In terms of the DUT outputs themselves, the degree of correlation has much to do with the internal topology of the device. While the analysis cannot be exhaustive here, one can consider two extremes. Suppose a packaged differential amplifier has noise dominant stages that are actually separate, single-ended amplifiers (left side of Figure 6). Assuming the dominant noise source within those stages is not some shared bias system, it is quite likely that the output noise will not be highly correlated.

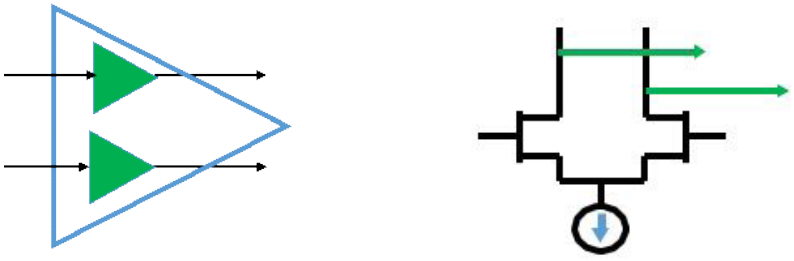

Figure 6. DUT Topology Influences Correlation of Noise Power Between Output Ports.

DUT topology has a large influence on the correlation of noise power between output ports. Separate dominant gain stages could make correlation negligible, but a dominant differential pair would do the opposite.

If, however, the dominant noise source is an output differential pair with much of the noise derived from a common source bias (right side of Figure 6), then the output noise will likely be highly correlated. Depending on one's knowledge of the DUT structure, it may be desirable to choose a measurement method that fits most closely. If not much is known, then doing the additional work to ensure correlation is treated correctly may be useful.

Uncorrelated and Single-Ended Measurements

If one can neglect correlation, the measurement is very simple and a straightforward extension of the 2-port DUT analysis. Two VNA receivers are used along with pre-amplification and filtering. A receiver calibration establishes an absolute power reference plane for the cold-source measurements. Note that for non-mmWave measurements (i.e., those made with the base VectorStar MS464XX VNA and not on the VectorStar ME7838X systems operating in broadband or mmWave mode), the b_1 and b_2 loops on the VNA proper are used for the noise inputs, even if a 4-port test set is being used. The instrument can remain in 4-port mode at all times, but the noise connections are not through that test set.

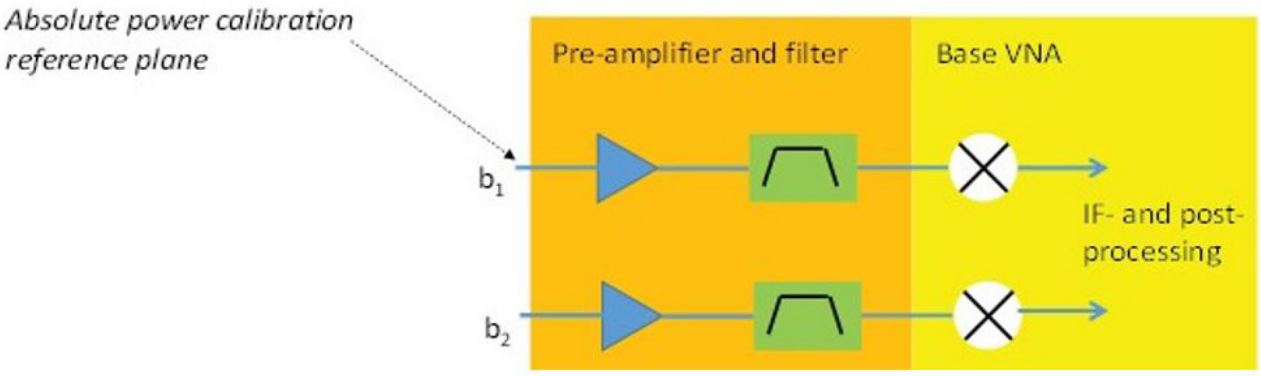

Figure 7. Configuration for Multiple Single-ended or Uncorrelated Noise Measurements.

For multiple single-ended or uncorrelated noise measurements, the configuration follows naturally from that for the 2-port DUTs.

The two paths need not be identical but must obey the same rules, as discussed in the VectorStar Measurement Guide (P/N 10410-00318 available on the Anritsu website), for overall gain and should have similar frequency responses in the measurement band of interest. Since correlation is neglected, the differential and common-mode noise power become simply

$$\overline{|b_d|^2} = \overline{|b_c|^2} = \frac{1}{2}\left(\overline{|b_1|^2} + \overline{|b_2|^2}\right) \tag{13}$$

The same concepts of receiver offset and network extraction tools discussed in Chapter 18 of the VectorStar Measurement Guide also apply here, except independent files can be loaded for each receiver. In the case of network extraction tools, a single .s4p file can be used where paths can be assigned to each receiver.

As a basic measurement example, consider a 3-port differential-output amplifier whose noise generators are known to be relatively uncorrelated. The uncorrelated method was chosen, and the receiver and noise calibrations performed. As seen in Figure 8 (traces 3 and 4), the common-mode and differential noise powers are the same as is forced by this method. The insertion gains for the two modes (derived from the . s3p file, using Eq. 6, for the DUT that was loaded) differ, however, by more than 20 dB (see traces 1 and 5). As a result, the noise figures (traces 2 and 6) also differ by more than 20 dB. The output of this particular device was well-matched, so the use of available gain would not have significantly changed the result.

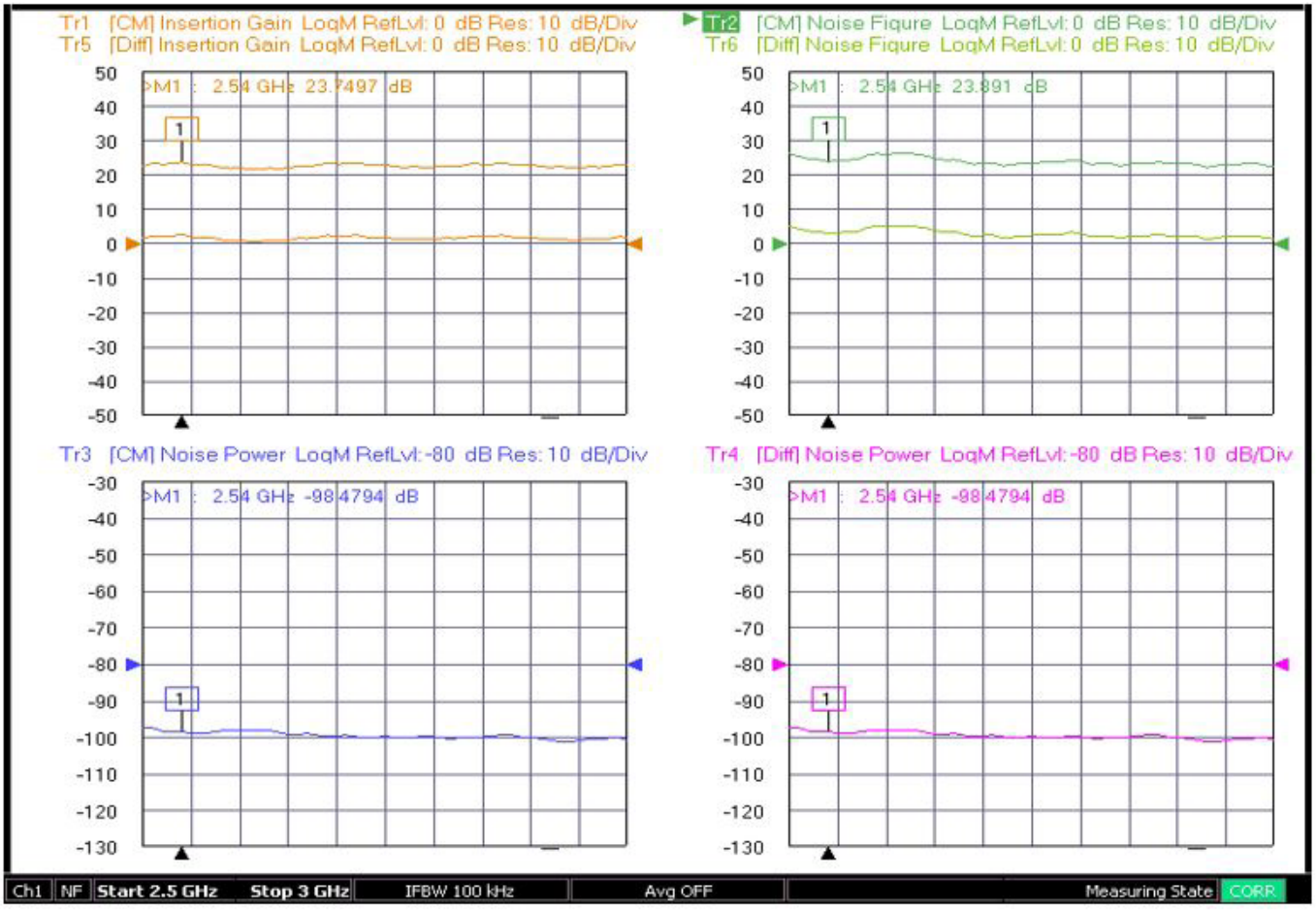

Figure 8. Three-port DUT with Uncorrelated Differential Output Measurement Example.

Although this method forces the differential and common-mode noise powers to be equal, the very different gains for the two modes cause the noise figures to also be quite different.

General calibration and measurement procedure:

- Setup composite receivers feeding b_1 and b_2.
- Perform a power calibration on port 1 (if desired) at a sufficiently low level that the composite receivers will not compress. Perform a receiver calibration (using this power calibration if desired) on both receiver paths. These calibrations can be done while in the noise figure application or can be recalled.
- Perform a noise calibration on both receiver paths with terminations attached to the receiver inputs.
- Load DUT S-parameter or gain data.
- Connect DUT and measure.

The various steps are illustrated in Figure 9 and Figure 10.

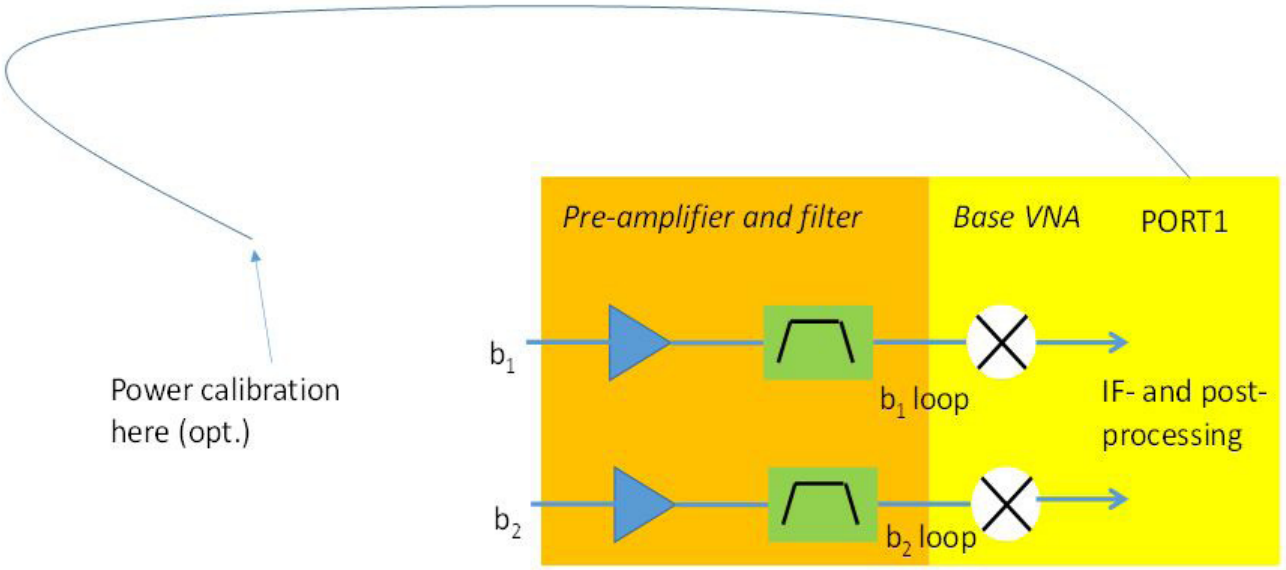

Figure 9. General Calibration and Measurement Steps (part 1).

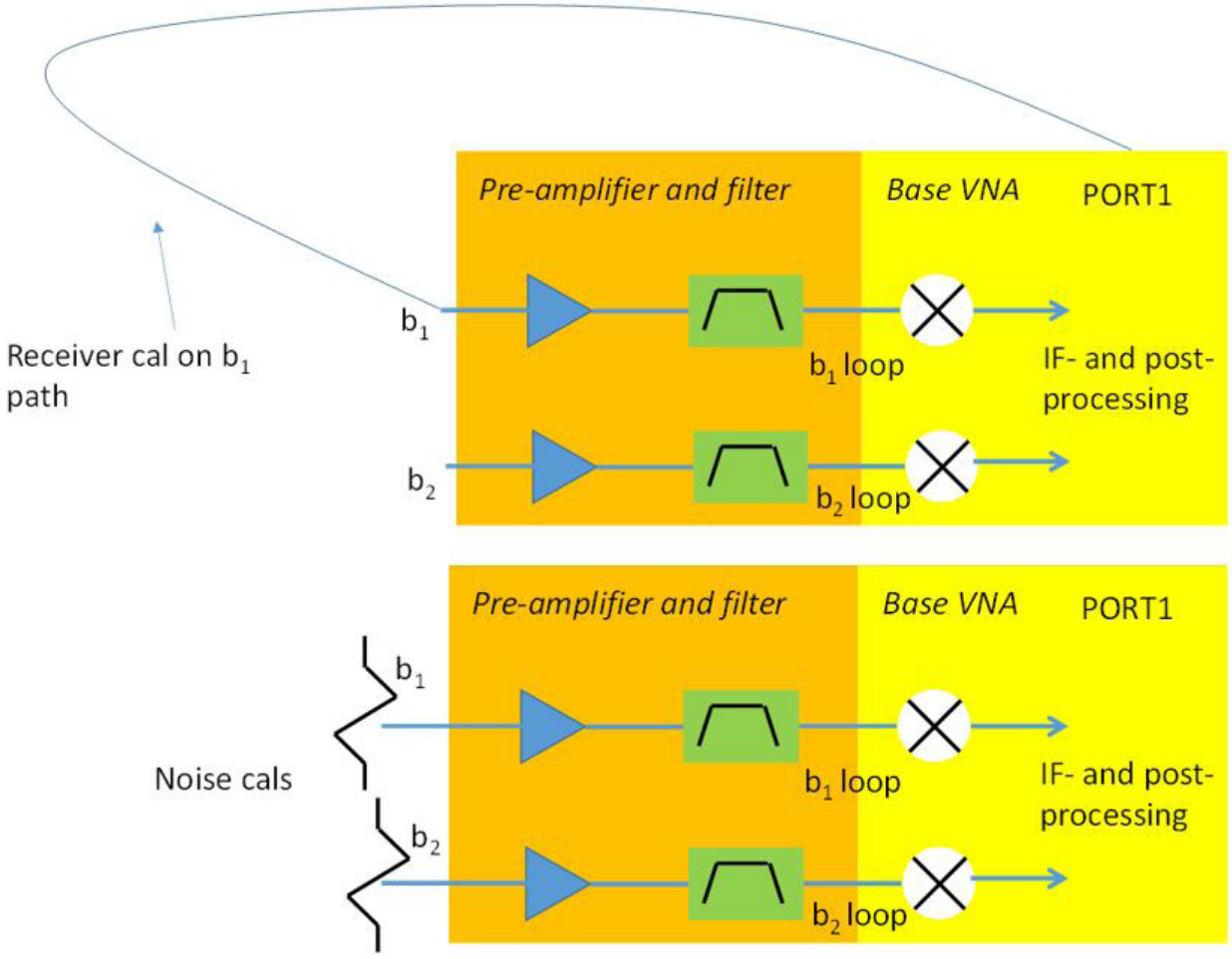

Figure 10. General Calibration and Measurement Steps (part 2).

Correlated Method and Coherent Receivers

Another method can take advantage of having multiple, time-coherent IF channels in the VNA to get at correlation between DUT output ports directly. Since the noise waveforms are directly digitized after IF processing, correlation between two noise signals can be maintained after certain levels of correction. This is the principle illustrated in Figure 11.

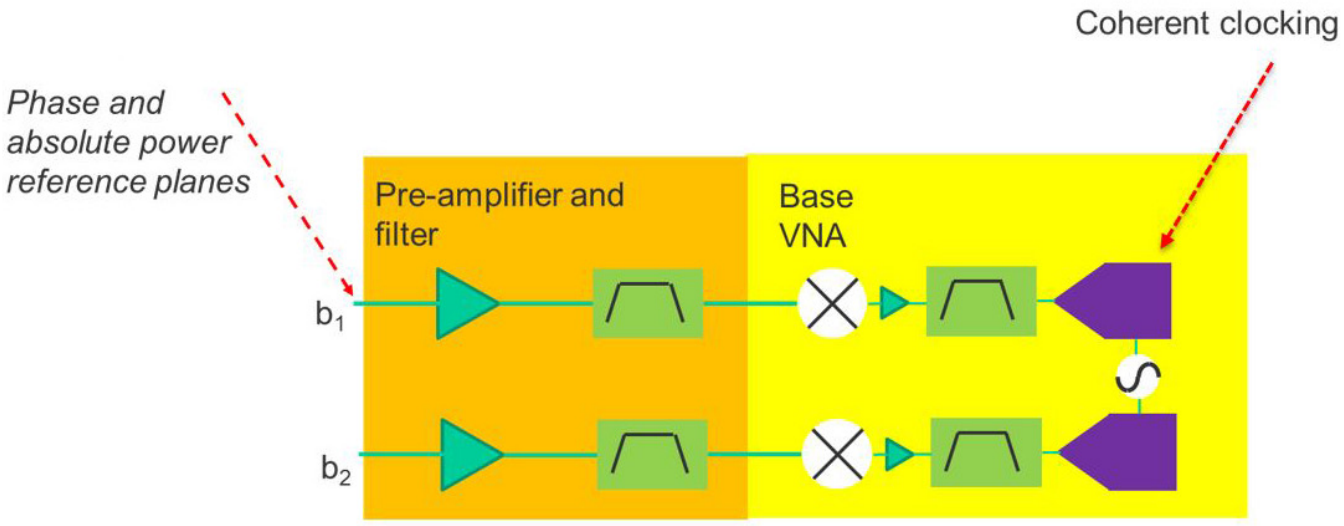

Figure 11. Correlated Noise Measurement Example Showing Coherent Digitizers.

In correlated noise measurements, the external hardware configuration is largely the same (see text) but coherent digitizers in the instrument are used to help directly identify the correlation levels.

If the correlation is directly measurable, then the differential and common-mode noise powers are

Of course, there are complications:

$$\overline{|b_d|^2} = \frac{1}{2}\left(\overline{|b_1|^2} + \overline{|b_2|^2}\right) - Re\left(\overline{b_1 \cdot b_2^*}\right)$$

$$\overline{|b_c|^2} = \frac{1}{2}\left(\overline{|b_1|^2} + \overline{|b_2|^2}\right) + Re\left(\overline{b_1 \cdot b_2^*}\right) \quad (14)$$

- The b_1 and b_2 measurements are now complex quantities, so a phase consistent reference plane must be established. The correlation calibration was established to achieve this using ratioed measurements against a deterministic signal from an internal source. A thru line connection to each receiver path is all that is required, and this can be done at the same time as a receiver calibration. As with the receiver calibrations, the system will interpolate/ (flat-line) extrapolate if the frequency range is different at measurement time vs. calibration time.
- At some point in a setup, coherence time can come into play. That is, two noise signals will only retain their coherence relative to each other over some finite length of line (even if well-matched). This is not necessarily intuitive, but is demonstrated in a more obvious way with the famous Michelson-Morely experiment (e.g., [8]) when performed with white light. In this experiment, two paths of different electrical lengths are made to interfere and create interference fringes. When the lengths get longer, these fringes get less distinct and eventually vanish when using broadband white light. The concept is that every source has some inherent coherence time that scales as 1/ (bandwidth) that describes the scale over which this occurs. For a VNA noise measurement, the bandwidth of relevance is the IF bandwidth of the measurement system, which is of order 1 MHz or smaller, so the length scales that could be a concern are longer than 1 microsecond.
- Even aside from coherence time, the receiver network itself can de-correlate a pair of incoming correlated noise signals. If the gain and noise generation of the receiver system greatly exceeds that of the DUT, the uncorrelated noise of the receiver system (assuming distinct amplifiers are being used) could wash out the signal correlation and this cannot be recovered. Through good practice, the receiver pre-amplifier chain should have just enough gain to pull the kTB base signal out

of the instrument floor. In addition, radically different electrical lengths of the receiver chains can de-correlate the signals in a periodic fashion, but the instrument uses the frequency response of the correlator calibration functions to partially correct for this. This correction relies on the frequency sweep being sufficiently wide relative to the electrical length delta, so adding some asymmetry to the setup is helpful for narrowband devices. If a CW frequency is being measured (or the frequency sweep is extremely narrow relative to the electrical length difference), a different algorithm will automatically activate that de-embeds receiver network correlation effects. However, accuracy is reduced mainly for the non-dominant mode (e.g., common-mode noise power for a differential amplifier will have reduced accuracy).

- Because of the use of frequency relationships, the data only updates at the end of sweep when in this mode.

As an example, consider the noise power from a passive DUT. From the earlier discussion, one would expect these to be uncorrelated and, in this measurement example, the differential and common-mode noise powers do essentially overlay (see the example in Figure 12). When a differential amplifier is measured (whose internal topology suggested a fair amount of noise correlation was likely), a very different result is obtained, as shown in Figure 13. Here the differential mode noise power exceeds the common-mode noise power by at least 10 dB (and by >20 dB at some frequencies). There is a lower limit to the correlated power measurement, set by the single-ended floor, so soft clipping will result in some measurements. In this particular case, the common-mode output impedance was such that even the thermal noise contribution to this mode was small at many frequencies.

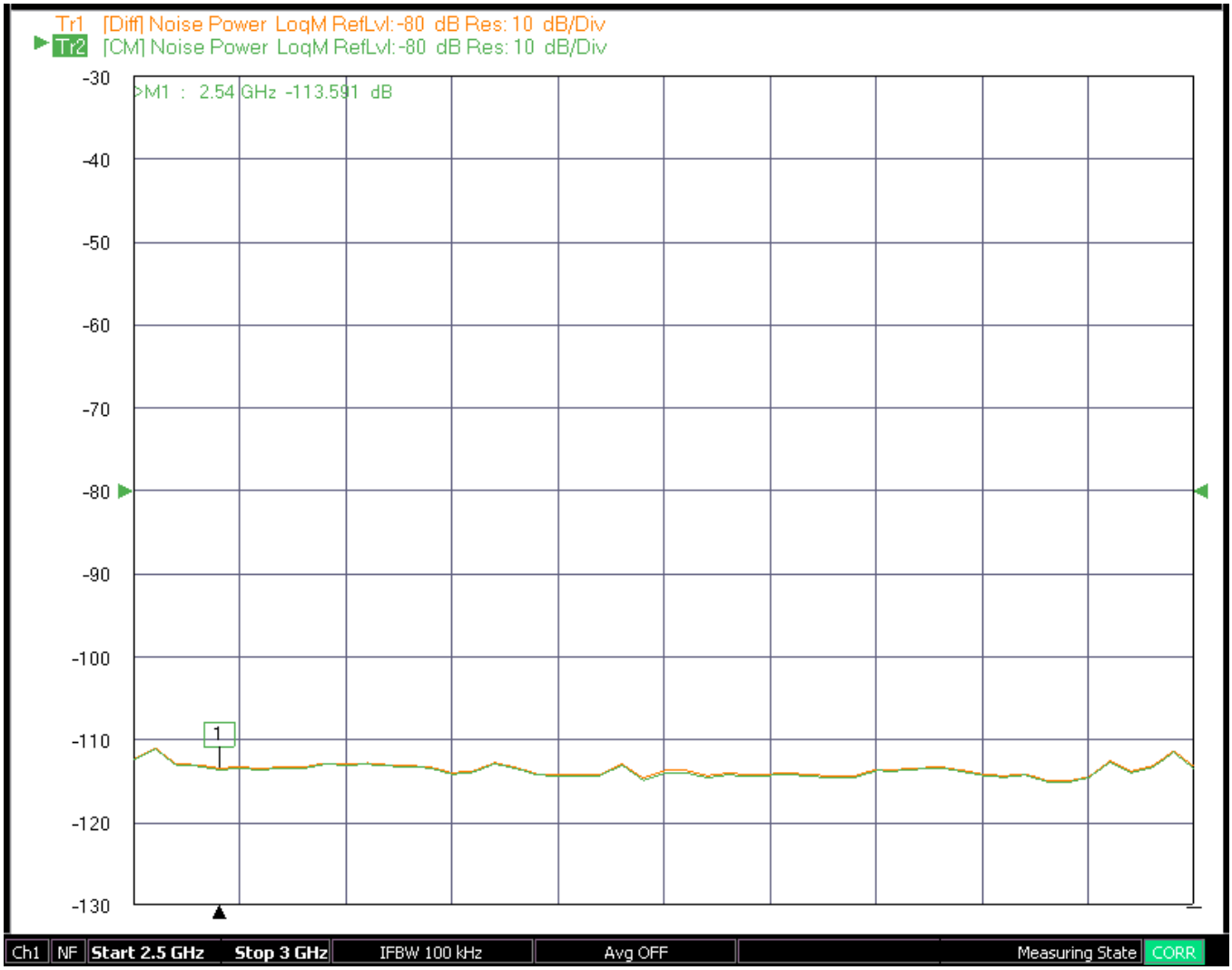

Figure 12. Correlated Noise Measurements Example for Passive DUT.

Correlated noise measurement examples are shown for a passive DUT in this figure and a differential amplifier in Figure 13.

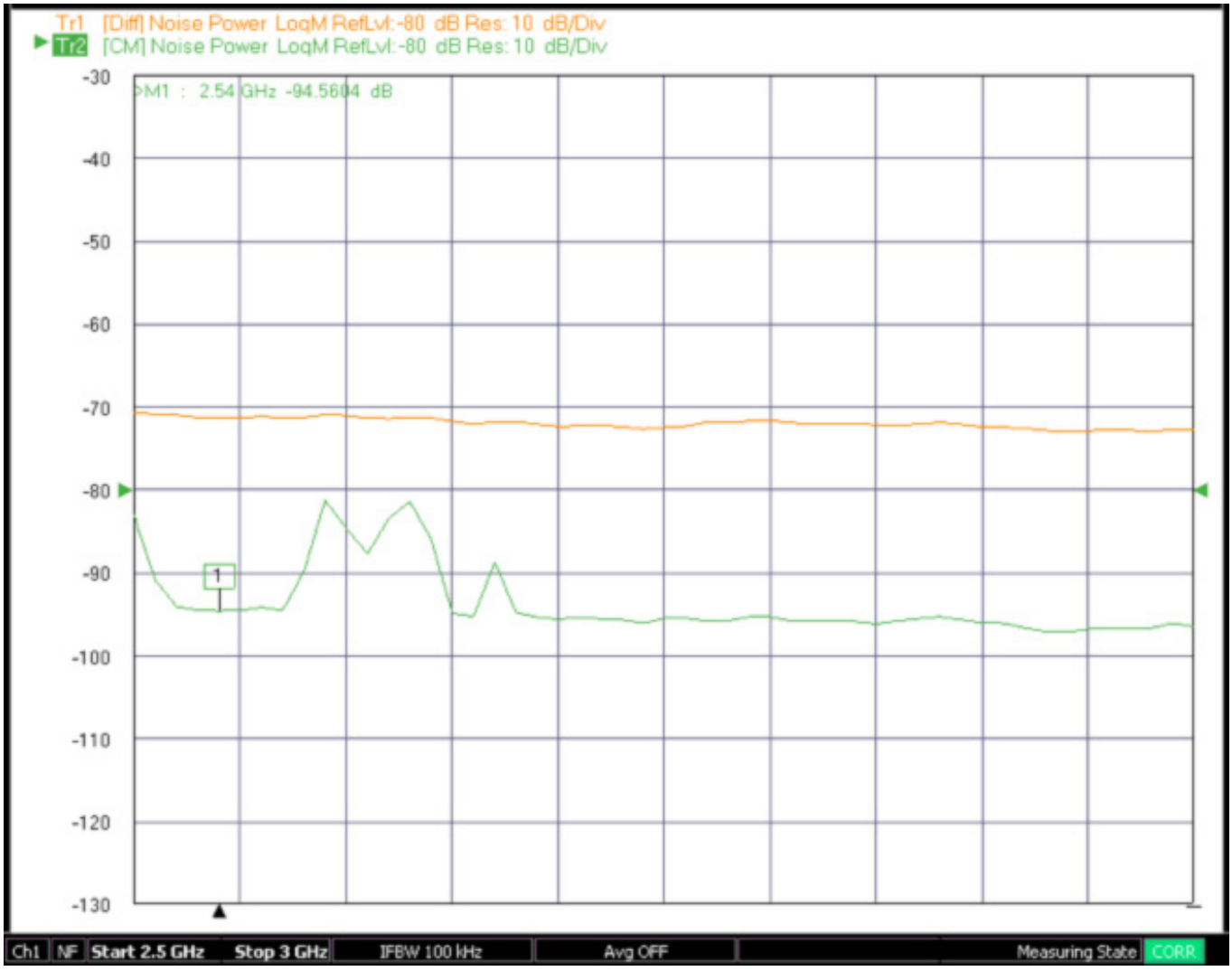

Figure 13. Correlated Noise Measurements for Differential Amplifier.

Correlated noise measurements examples are shown for a passive DUT in Figure 12 and a differential mplifier in this figure.

General calibration and measurement procedure:

- Setup composite receivers feeding b_1 and b_2.
- Perform a power calibration on port 1 (if desired) at a sufficiently low level that the composite receivers will not compress. Perform a receiver calibration (using this power calibration, if desired) and correlation calibrations on both receiver paths (the receiver and correlation calibrations can be done simultaneously using the checkbox in the CALIBRATION dialog). These calibrations can be done while in the noise figure application or can be recalled.
- Perform a noise calibration on both receiver paths with terminations attached to the receiver inputs.
- Load DUT S-parameter or gain data.
- Connect DUT and measure.

The steps are essentially the same as in Figure 10 since the receiver and correlation calibrations can be done with the same connection. A checkbox in the CALIBRATION dialog allows the two calibrations to execute simultaneously.

Balun-Based Methods and Handling of Imperfections

A more classical approach to dealing with correlated DUT noise outputs is to send them first to a balun (or a combiner in more general terms). If the line lengths to the balun are equal and the balun balance is ideal, then a differential signal is generated for conventional 2-port noise analysis and only the insertion loss of the balun must be de-embedded (e.g., [5]-[6]).

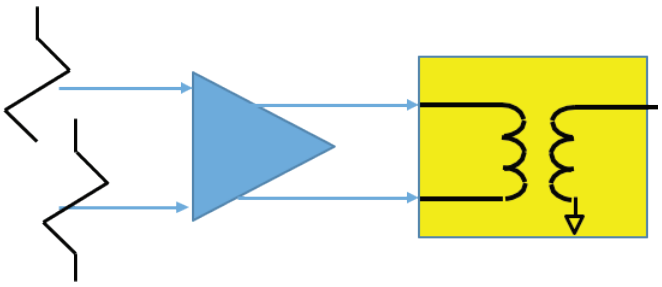

Figure 14. Using a Balun for Differential Noise Figure Measurements.

The use of a balun (or combiner more generically) is a useful measurement method to get differential (or common-mode) noise figure when coupled with de-embedding.

If the balance of the combiner/balun is less than ideal, some errors can be introduced. On a simple level, for noise figure, the gain of the balun is described by Sd1, so asymmetries will be corrected directly. Noise power, however, is also affected. Similar to the discussion in the previous section, the difference between correlated and uncorrelated noise power is the correlation term. One measure of the effect of balun irregularities may then be the change they introduce into the correlation term. A simulation was run where varying degrees of imbalance were inserted and the fractional change in the correlation term was computed (see results in Figure 15). Relatively large amounts (up to 1 dB) of amplitude imbalance did relatively little, but 10 degrees of phase imbalance caused about ~0.5 dB noise figure error. At least for high-frequency broadband baluns, such a level of imbalance is not unusual. Considering also the lines connecting the DUT to the balun (assuming they are not integrated on the same chip, in which case this can indicate the sensitivity to layout): 10 degrees of phase difference at 70 GHz corresponds to about 120 µm length difference with an air dielectric (and less on any substrate). Thus, some means of correcting for imbalance might have a detectable effect on overall measurement accuracy.

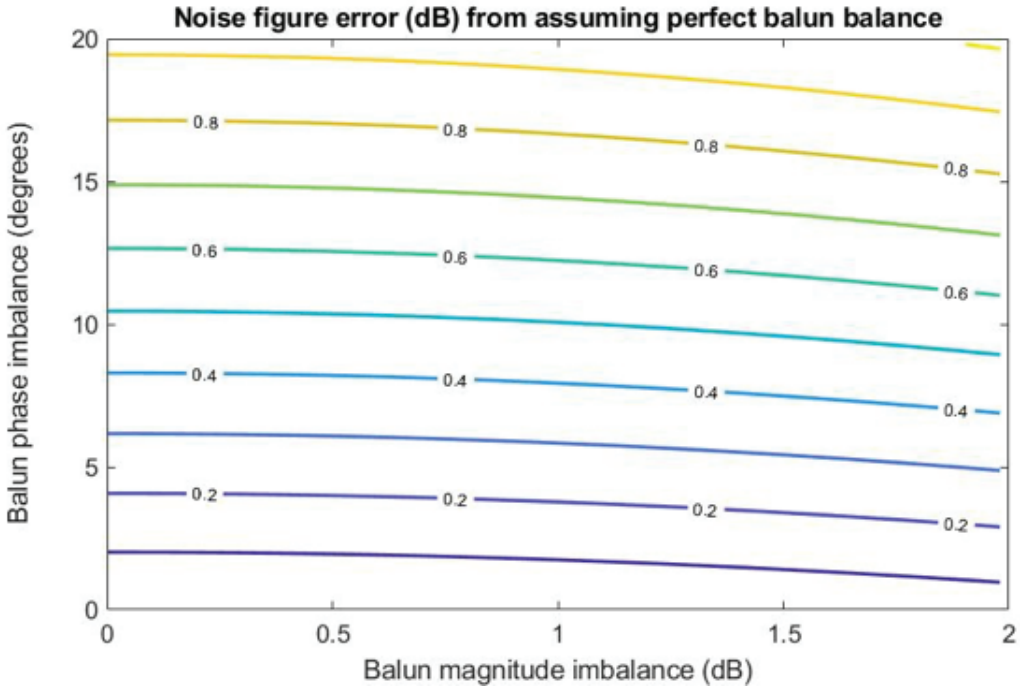

Figure 15. Noise Figure Error from Neglecting Balun Imbalance.

The calculations assume minimal ohmic balun insertion loss and neglect mismatch.

Conceptually, one can arrive at the correlation term by separately measuring the single-ended noise powers from the DUT and removing their effects after propagating them through the S-parameters of the balun (e.g., [7]). This does leave one additional layer of ambiguity on how the noise powers combine in the balun, since the real and imaginary parts of correlation can co-mingle. If one can assume that the imaginary part is negligible, only one balun-based measurement (to update the display real time) is required. To fully treat the imaginary part, a second swapped measurement with the balun in place can be done. This swapped measurement is stored, much like a noise calibration step, and should be updated with DUT changes. In both cases (with or without the swapped measurement), the single-ended DUT noise measurements must be stored, also like noise calibration steps, and these should also be refreshed with DUT changes. The sequence of measurements is shown in Figure 16.

Some notes on this measurement:

- The balun (combiner) must be pre-characterized and an .s3p file stored with port 3 as the defined common port. A port swap tool is available for files stored with some other port configuration. Interpolation and (flat line) extrapolation will be used for frequency lists that do not match the current list.
- Step 2 (and 3 if the second combiner measurement is used) should be repeated if the DUT or its bias state is changed.
- Only the b_2 receiver chain is used for the combiner measurements. While the b_1 receiver is used for the single-ended measurements, the same pre-amplifier/filter assembly can be used on b_1 and b_2 inputs since these single-ended measurements do not have to be performed simultaneously.

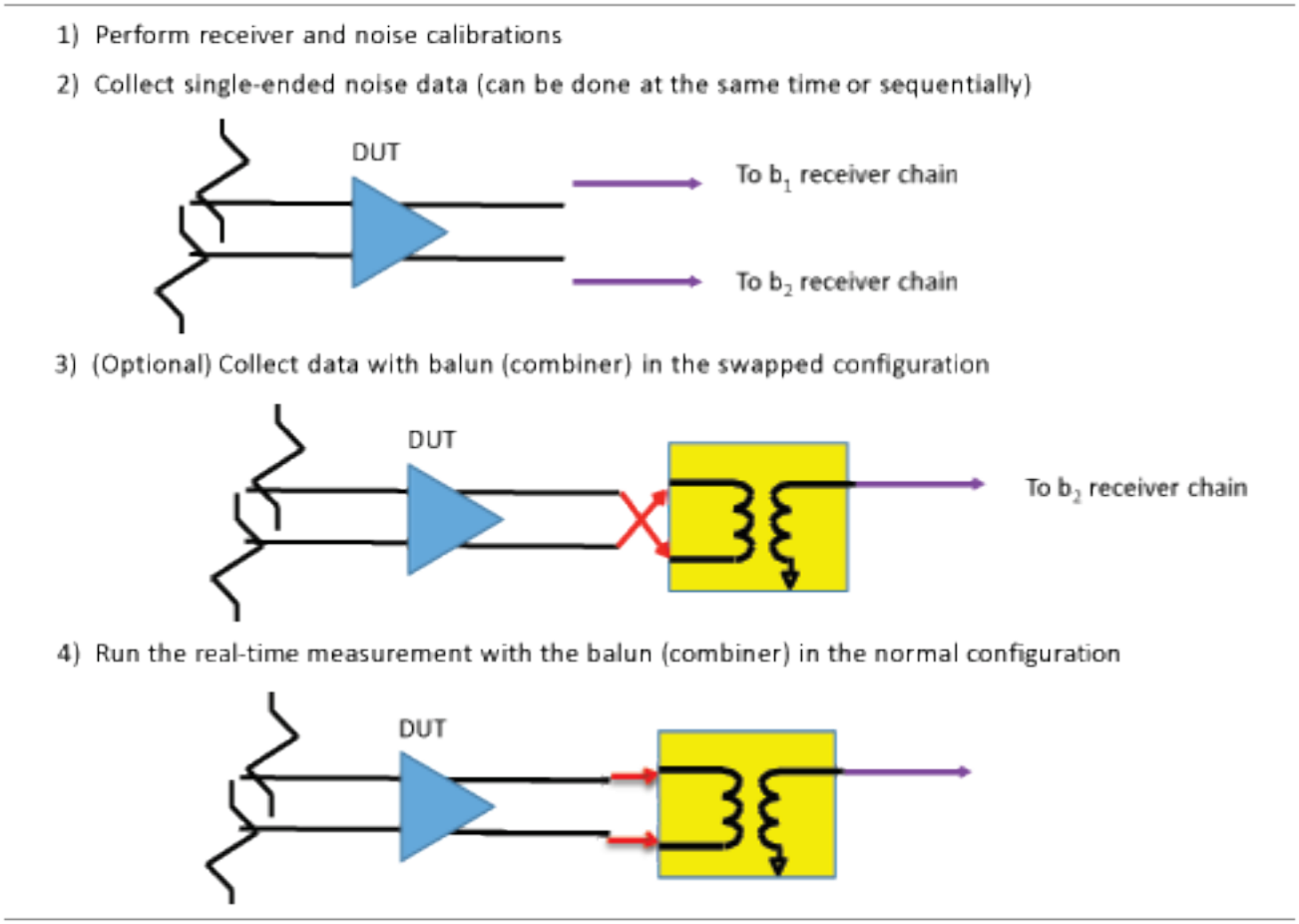

Figure 16. Measurement Sequence for the Combiner Method

Step 3 is optional when the double-combiner measurement sub-method is selected, but can improve accuracy, particularly for DUTs with partially correlated outputs.

- There are no particular constraints on the balun parameters, but if the insertion loss is very high, low DUT noise figures (or moderate noise figures on very low gain DUTs) may have higher uncertainties. The algorithm has to work harder the more non-ideal the balun/combiner is, so the characterization accuracy of that balun becomes more important in those cases.

Consider an example measurement that uses the full characterization of the combiner to calculate the correlation, as just discussed. The resulting noise power is plotted in Figure 17, where it is contrasted with a measurement where the noise power was just measured directly and the loss (in a differential sense) of the combiner simply de-embedded. Note that gain definitions do not play a role in these plots, as it is simple noise power referenced to a common reference plane (and de-embedding would not be able to treat correlation differences). But the errors do reach 0.5 dB or more in places, which is not entirely inconsistent with Figure 15. The net amount of difference is a function of both the non-idealities in the combining structure and the degree of correlation in this particular DUT output. As always, noise power (in excess of calibration values) will propagate to noise figure on a dB-for-dB basis.

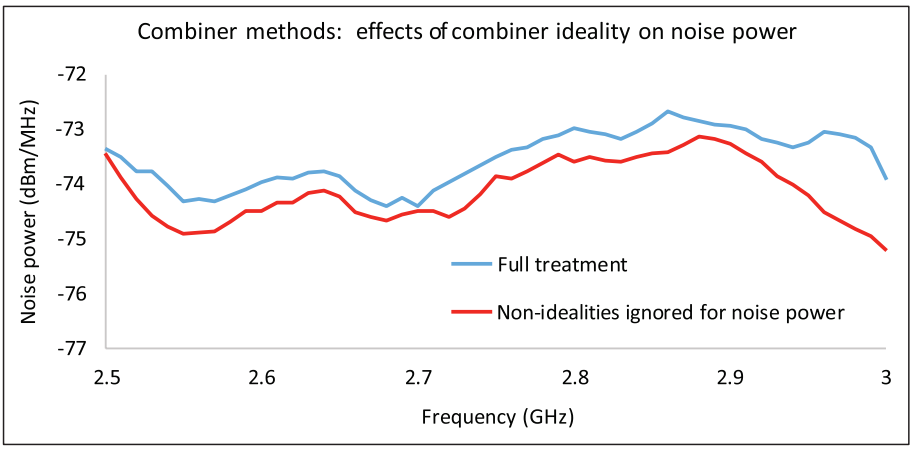

Figure 17. Noise Power Examples using Balun and Classical Combiner Approaches.

An example measurement result of noise power for a differential amplifier using the balun (combiner) method of this section (blue/upper trace), and for a more classical combiner approach (red/lower trace) where the noise power from the combiner is measured directly and the loss of the balun de-embedded.

The effect of using the single or double combiner measurement can be more subtle depending on the details of the DUT correlation. A relatively representative example measurement of a highly correlated DUT is shown in Figure 18 for both approaches to incorporate balun non-idealities. The average difference over the bandwidth was ~0.3 dB, which is higher than the repeatability level for this DUT measurement (~0.1 dB) but less than the absolute uncertainty levels and less than the differences seen in Figure 17 (where the balun was treated as ideal for correlation purposes). There may be devices with different correlation structures where the single/double difference could be larger.

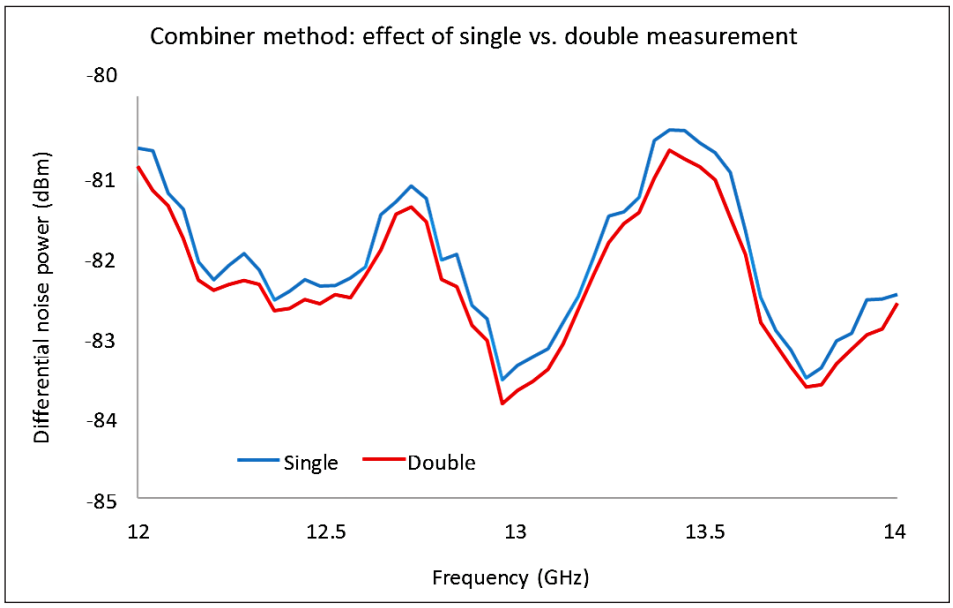

Figure 18. Noise Power Examples Using Balun and Single Combiner Methods.

An example measurement result of noise power for a differential amplifier using the balun (combiner) method of this section, and a single combiner/balun measurement (blue), or the double measurement (red), which makes fewer assumptions about the nature of the correlation function..

To re-iterate, the general procedure can be described by (see Figures 9 and 10):

- Setup composite receivers feeding b_1 and b_2.
- Perform a power calibration on port 1 (if desired) at a sufficiently low level that the composite receivers will not compress. Perform a receiver calibration (using this power calibration if desired) on both receiver paths (the receiver and correlation calibrations can be done simultaneously using the checkbox in the dialog). These calibrations can be done while in the noise figure application or can be recalled.
- Perform a noise calibration on both receiver paths with terminations attached to the receiver inputs.
- Load DUT S-parameter or gain data.
- Connect DUT (without the combiner/balun present) and collect b_1 and b_2 noise data (can be done at the same time).
- If the double combiner measurement was selected, connect the combiner/balun with the inputs swapped
  (relative to the desired connection) and collect the data. If single was selected, skip this bullet.
- Connect DUT and combiner/balun and measure.

Measurement Uncertainty

Since at its core, a noise figure measurement discussed here is a combination of a noise power measurement and analysis of DUT gain, many of the uncertainty components are the same as for single-ended noise figure. Some of these elements are:

- Accuracy of DUT gain. This is an S-parameter uncertainty problem, but in this example it may involve those derived from 4-port measurements. The contributing factors are the same and the S-parameter uncertainties are described in great length elsewhere.
- Power and receiver calibration accuracy. Since a cold-source method is used for the differential noise figure measurements as well, how the power reference plane is established matters.
- System noise floor and having adequate gain (and noise figure) in the DUT and composite receiver is essential to getting the noise power in a linear range for the VNA analog-to-digital converters.
- Sufficient RMS points per frequency to keep measurement jitter tolerable.

Specifically for differential noise figure (aside from the slightly different gain computations and net uncertainties in those terms), there is the context of the measurement that is important: defined with uncorrelated noise inputs at temperature T_0 and all terminations are reflection-less. While not that different from the 2-port assumptions, there are more places for changes to happen in the setup. There is then the topic of correlation between DUT outputs that has been a central topic here. The previous section showed the scale of errors in neglecting correlation in balun (combiner)-based methods and there is an uncertainty contribution from the S-parameter measurements of the balun. In the case of the direct correlation method, there is an S-parameter-like term embedded in the correlation calibration (how accurately can the phase reference plane be established, which will be affected by port match, etc.) and from the ability to correct for receiver-network-induced de-correlation (which will depend on relative gain levels and electrical length differences).

More generally, the effect can be somewhat self-evident by looking at Eq. 14. Using arbitrary scaling, suppose the average of single-ended noise powers was 1 linear unit. If the DUT outputs are completely uncorrelated, the common-mode and differential noise powers will also be 1 linear unit. At the limit of full correlation, they could reach values of 0 and 2 respectively (or the other way around for a common-mode amplifier), so the percentage or dB errors can be extreme, theoretically. In practice, this is usually not the case, however the potential errors may be useful to understand (and, indeed, one often does not care as much about common-mode noise figure since the gains are so low; there are also additional uncertainty complications with the lower noise power since the subtraction of nearly equal numbers is involved).

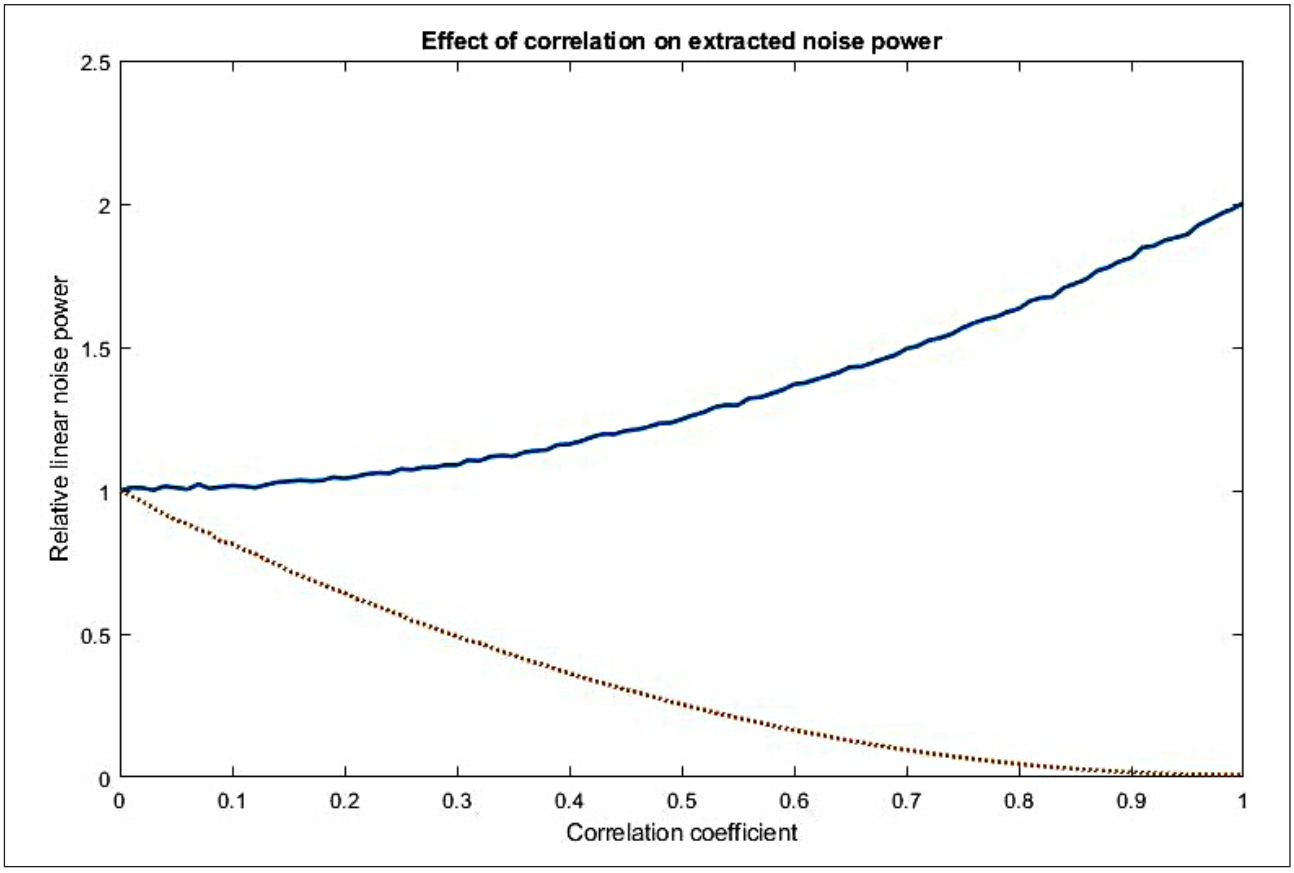

Figure 19. Monte-Carlo Simulation of Extracted Noise Powers for Different Levels of Correlation.

A Monte-Carlo simulation of extracted noise powers for different levels of correlation for the differential (blue/top)) and common-modes (red/bottom), assuming a differential amplifier. The end points of the curves are easy to understand on an ideal level.

Other Comments

Differential noise figure is compatible with the broadband and mmWave systems and, as with option 41, a receiver module greatly helps this effort by removing coupler losses (as loops are not available in the mmWave bands). Two such modules (like the 3744A-Rx) are required for most of the differential noise figure measurements and receiver offset corrections can be applied to both receiver paths. In a 4-port setup, these receiver modules should be connected as ports 2 and 4, as these will be the only paths monitored for noise measurements. Port 1 can remain as a standard module, as it will be used for receiver and correlation calibrations. The overall calibration processes follow from what has been discussed.

References

1. H. T. Friis, “Noise figure of radio receivers,” Proc. IRE, vol. 32, Jul. 1944, pp. 419-422.
2. “Noise Figure”, Anritsu Application Note 11410-00210, Aug. 2000.
3. D. Vondran, “Noise figure measurement: corrections related to match and gain,” Microwave Journal, Mar. 1999, pp. 22-38.
4. N. Otegi, J. M. Collantes, and M. Sayed, “Cold-source measurements for noise figure calculation in spectrum analyzers,” 67th ARFTG Conf. Dig., Jun. 2006, pp. 223-228.
5. N. Otegi, J. M. Collantes, and M. Sayed, “Receiver noise calibration for vector network analyzer,” 76th ARFTG Conf. Dig., Dec. 2010, pp. 1-5.
6. J. M. Collantes, R. D. Pollard, and M. Sayed, “Effects of DUT mismatch on the noise figure characterization: A comparative analysis of two Y-factor techniques,” IEEE Trans. Instr. And Meas., vol. 51, Dec. 2002, pp. 1150-1156.
7. L. Escotte, R. Plana, and J. Graffeuil, “Evaluation of noise parameter extraction methods,” IEEE Trans. Micr. Theory Tech., vol. 41, Mar 1993, pp. 382-387.
8. “Supplement 1 to the “Guide to the expression of uncertainty in measurement” — Propagation of distributions using a Monte Carlo method”, Joint Committee for Guides in Metrology, 2008.
9. J. Randa, “Noise characterization of multiport amplifiers,” IEEE Trans. Micr. Theory Techn., vol. 49, pp.1757-1763, Oct. 2001.
10. S. Wedge and D. Rutledge, “Noise waves and passive linear multiports,” IEEE Micr. Guid. Wave Lett., vol. 1, pp. 117-119, May 1991.
11. L. Boglione, “Generalized determination of device noise parameters,” IEEE Trans. Micr. Theory Techn., vol. 65, pp. 4014-4025, Oct. 2017.
12. Y. Chang, S. Lin, H. Liao, H. Chiou, and Y. Juang, “On-wafer differential noise figure and large signal measurements of low-noise amplifier,” Proc. 39th Eur. Micr. Conf., Oct. 2009, pp. 699-702.
13. J. Dunsmore and S. Wood, “Vector corrected noise figure and noise parameter measurements of differential amplifiers,” Proc. 39th Eur. Micr. Conf., Oct. 2009, pp. 707-710.
14. M. Robens, R. Wunderlich, and S. Heinen, “Differential noise figure de-embedding: a comparison of available approaches,” IEEE Trans. Micr. Theory Techn., vol. 59, pp. 1397-1407, May 2011.
15. Y. Andee, C. Arnaud, F. Graux, and F. Danneville, “De-embedding differential noise figure using the correlation of noise output waves,” 84th ARFTG Conf. Dig., Dec. 2014, pp. 1-4.
16. A. A. Michelson and E. W. Morley, "On the relative motion of the earth and the luminiferous ether".
17. American Journal of Science, vol. 34, pp. 333–345, Dec. 1887.

Anritsu envision : ensure

Specifications are subject to change without notice.

• United States
Anritsu Company
450 Century Parkway, Suite 190, Allen, TX 75013 U.S.A.
Toll Free: +1-800-267-4878
Phone: +1-972-644-1777

• Canada
Anritsu Electronics Ltd.
700 Silver Seven Road, Suite 120,
Kanata, Ontario K2V 1C3, Canada
Phone: +1-613-591-2003
Fax: +1-613-591-1006

• Brazil
Anritsu Electrônica Ltda.
Praça Amadeu Amaral, 27 - 1 Andar
01327-010 - Bela Vista - Sao Paulo - SP - Brazil
Phone: +55-11-3283-2511
Fax: +55-11-3288-6940

• Mexico
Anritsu Company, S.A. de C.V.
Blvd Miguel de Cervantes Saavedra #169 Piso 1, Col. Granada
Mexico, Ciudad de Mexico, 11520, MEXICO
Phone: +52-55-4169-7104

• United Kingdom
Anritsu EMEA Ltd.
200 Capability Green, Luton, Bedfordshire LU1 3LU, U.K.
Phone: +44-1582-433280
Fax: +44-1582-731303

• France
Anritsu S.A.
12 avenue du Québec, Batiment Iris 1-Silic 612,
91140 Villebon-sur-Yvette, France
Phone: +33-1-60-92-15-50
Fax: +33-1-64-46-10-65

• Germany
Anritsu GmbH
Nemetschek Haus, Konrad-Zuse-Platz 1
81829 München, Germany
Phone: +49-89-442308-0
Fax: +49-89-442308-55

• Italy
Anritsu S.r.l.
Via Elio Vittorini 129, 00144 Roma Italy
Phone: +39-06-509-9711
Fax: +39-06-502-2425

• Sweden
Anritsu AB
Isafjordsgatan 32C, 164 40 KISTA, Sweden
Phone: +46-8-534-707-00

• Finland
Anritsu AB
Teknobulevardi 3-5, FI-01530 VANTAA, Finland
Phone: +358-20-741-8100
Fax: +358-20-741-8111

• Denmark
Anritsu A/S
Kay Fiskers Plads 9, 2300 Copenhagen S, Denmark
Phone: +45-7211-2200
Fax: +45-7211-2210

• Russia
Anritsu EMEA Ltd.
Representation Office in Russia
Tverskaya str. 16/2, bld. 1, 7th floor.
Moscow, 125009, Russia
Phone: +7-495-363-1694
Fax: +7-495-935-8962

• Spain
Anritsu EMEA Ltd.
Representation Office in Spain
Edificio Cuzco IV, Po. de la Castellana, 141, Pta. 5
28046, Madrid, Spain
Phone: +34-915-726-761
Fax: +34-915-726-621

• United Arab Emirates
Anritsu EMEA Ltd.
Dubai Liaison Office
P O Box 500413 - Dubai Internet City
Al Thuraya Building, Tower 1, Suite 701, 7th floor
Dubai, United Arab Emirates
Phone: +971-4-3670352
Fax: +971-4-3688460

• India
Anritsu India Pvt Ltd.
6th Floor, Indiqube ETA, No.38/4, Adjacent to EMC2,
Doddanekundi, Outer Ring Road, Bengaluru – 560048, India
Phone: +91-80-4058-1300
Fax: +91-80-4058-1301

• Singapore
Anritsu Pte. Ltd.
11 Chang Charn Road, #04-01, Shriro House
Singapore 159640
Phone: +65-6282-2400
Fax: +65-6282-2533

• P. R. China (Shanghai)
Anritsu (China) Co., Ltd.
27th Floor, Tower A,
New Caohejing International Business Center
No. 391 Gui Ping Road Shanghai, Xu Hui Di District,
Shanghai 200233, P.R. China
Phone: +86-21-6237-0898
Fax: +86-21-6237-0899

• P. R. China (Hong Kong)
Anritsu Company Ltd.
Unit 1006-7, 10/F., Greenfield Tower, Concordia Plaza,
No. 1 Science Museum Road, Tsim Sha Tsui East,
Kowloon, Hong Kong, P. R. China
Phone: +852-2301-4980
Fax: +852-2301-3545

• Japan
Anritsu Corporation
8-5, Tamura-cho, Atsugi-shi,
Kanagawa, 243-0016 Japan
Phone: +81-46-296-6509
Fax: +81-46-225-8352

• Korea
Anritsu Corporation, Ltd.
5FL, 235 Pangyoyeok-ro, Bundang-gu, Seongnam-si,
Gyeonggi-do, 13494 Korea
Phone: +82-31-696-7750
Fax: +82-31-696-7751

• Australia
Anritsu Pty Ltd.
Unit 20, 21-35 Ricketts Road,
Mount Waverley, Victoria 3149, Australia
Phone: +61-3-9558-8177
Fax: +61-3-9558-8255

• Taiwan
Anritsu Company Inc.
7F, No. 316, Sec. 1, Neihu Rd., Taipei 114, Taiwan
Phone: +886-2-8751-1816
Fax: +886-2-8751-1817

11410-01094, Rev. A Printed in United States 2018-11